Appl. Phys. 14, 255–268 (1977)

Applied Physics

Modulation Behavior of Semiconductor Injection Lasers

G. Arnold and *P. Russer*
AEG-Telefunken, Forschungsinstitut, D-7900 Ulm, Fed. Rep. Germany

Received 19 April 1977/Accepted 27 June 1977

Abstract. GaAs double heterostructure semiconductor injection lasers which now exhibit more than 25000 h cw room temperature lifetime are of great interest for future use as directly modulated transmitters for high bit-rate fiber optical communications. The effects limiting this application are modulation distortions, spectral width and additional spectral broadening in the case of modulation and spontaneous fluctuations of the output power. The dynamic and spectral behavior of injection lasers, the methods of high bit-rate modulation and the improvement of the high bit-rate modulation capability by coupling two lasers are discussed.

PACS Codes: 42.80, 42.55, 85.60

Semiconductor injection lasers are of great interest as transmitters for high bit-rate fiber optical communication systems [1, 2]. The main advantages of semiconductor injection lasers are simple construction, small dimensions, high efficiency and direct modulation capability up to the GHz range. Semiconductor injection lasers yield a good coupling efficiency also into monomode fibers [3] and for their narrow emission spectrum only a low pulse broadening due to fiber dispersion when monomode fibers are used. At the wavelength of GaAs injection lasers the dispersion of usual monomode fibers is $1\,\mathrm{ns\,km^{-1}}$ for 1% relative optical bandwidth [4, 5].

Considerable effort has been undertaken in recent years to develop cw lasers with long lifetimes at room temperature. Today lifetimes up to 25000 h have been achieved [6, 7]. Several review papers on semiconductor injection lasers have been written [8–12]. In this paper we shall discuss the modulation and spectral properties of double heterostructure (DHS) stripe geometry $GaAs/Ga_{1-x}Al_xAs$ injection lasers for cw room temperature operation. We suppose that other semiconductor materials as, for example, $InP/Ga_xIn_{1-x}As_yP_{1-y}$ shall gain importance in the future [13, 14] but until now no information about the modulation behavior of these laser types is reported.

For high bit-rate communication from several 100 Mbit/s up into the Gbit/s-range, lasers must have the following properties:

(i) No modulation distortions (pattern effects).
(ii) A narrow spectral bandwidth.
(iii) No high spectral broadening due to direct modulation.
(iv) No spontaneous fluctuations.

The rate equations which describe the dynamic behavior of injection lasers are discussed in detail in the first section. In the further sections we review and discuss the modulation, spectral and fluctuation behavior of injection lasers, and the methods for direct modulation at high bit-rates.

1. The Rate Equations

Semiconductor injection lasers exhibit a very complex dynamic behavior. Until now not all experimentally observed effects can be explained satisfactorily, but for the main properties a good theoretical understanding has been achieved. The dynamics of a semiconductor injection laser is governed by rate equations [15–22]. The quantum mechanical rate equations for the electron density and polarisation operators and the photon amplitude operators give informations about the time development of the photon amplitude, frequency and

phase and also about the statistical properties due to quantum fluctuations [15, 18, 19, 21]. In many cases, where only the time dependence of the photon number mean value is of interest and an interaction of modes with a very narrow wavelength spacing does not occur, the analysis can be performed by the much simpler classical rate equations for the electron density in the active layer and the photon numbers in the modes [16, 17, 20, 22]. Due to the intraband scattering processes spectral hole burning is unimportant in injection lasers and the cause for the mainly observed multimode operation of injection lasers is assumed to be spatial hole burning [23–25]. We give multimode rate equations for the electron density and photon numbers. In the multimode case the inhomogeneous distribution of electron and photon densities must be taken into account. For an active layer, parallel to the $x-y$-plane with a thickness d, these rate equations are

$$\frac{\partial n(x,y,t)}{\partial t} = \frac{J(x,y,t)}{e_0 d} - \frac{1}{\varkappa} R_{sp}(n) + D\nabla^2 n(x,y,t) - \frac{1}{d}\sum_i \frac{\Gamma_i}{\Phi(E_i)} S_i(t)|\varphi_i(x,y)|^2 r_{st}(E_i,n) \tag{1}$$

$$\frac{\partial S_i(t)}{\partial t} = -\frac{S_i(t)}{\tau_{phi}} + \frac{\Gamma_i}{\Phi(E_i)}\int |\varphi_i(x,y)|^2 r_{sp}(E_i,n)dxdy + \frac{\Gamma_i}{\Phi(E_i)} S_i(t)\int |\varphi_i(x,y)|^2 r_{st}(E_i,n)dxdy. \tag{2}$$

The electron density n depends on x and y and is assumed to be confined within the active layer and constant therein in z direction. J is the injection current density, e_0 the absolute value of the electron charge. S_i is the photon number in the i-th mode, $\varphi_i(x,y)$ is the normalized scalar complex photon amplitude function. The complex amplitude function is normalized so that $|\varphi_i(x,y)|^2$ integrated over the whole $x-y$-plane yields 1. Γ_i is the photon confinement factor which gives the ratio of photon energy concentrated within the active layer of volume V to the total photon energy, both for the i-th mode [12]. The stimulated and spontaneous emission rates per unit of volume and unit of photon energy r_{st} and r_{sp} have been calculated by Lasher and Stern [26] for GaAs at room temperature, assuming transitions between parabolic bands with k selection rule for pure material and without k selection rule for highly doped material. For parabolic bands without k selection rule, and additional Gaussian impurity band tails calculations have been performed by Casey and Stern [27]. For transitions between parabolic bands without k selection rule an approximate expression for r_{st} has been given by Marinelli [28]. R_{sp} is the total spontaneous emission rate per unit of volume, and $\varkappa$ is the internal quantum efficiency. $\Phi(E_i)$ is the number of modes per unit of volume and unit of energy and is given by

$$\Phi(E_i) = \frac{\bar{n}_i' \bar{n}_i^2 E_i^2}{\pi^2 \hbar^3 c^3}, \tag{3}$$

where $\bar{n}_i$ is the index of refraction for the i-th mode, and the effective index of refraction $\bar{n}_i'$ considering the dispersion is given by

$$\bar{n}_i' = \bar{n}_i\left(1 - \frac{\lambda_i}{\bar{n}_i}\frac{\partial \bar{n}_i}{d\lambda_i}\right). \tag{4}$$

For a vacuum wavelength of 8500 Å we obtain $E_i = 1.46$ eV and with $\bar{n} = 3.6$ and $\bar{n}' \approx 5$ [29] the number of modes per unit of volume and unit of energy is $\Phi(E_i) = 1.817 \times 10^{12}\,\mathrm{meV^{-1}\,cm^{-3}}$. D is the diffusion constant and can be calculated from $D = \mu_n kT/e_0$ (where μ_n is the electron mobility, k the Boltzman constant and T the absolute temperature) or from $D = L_n^2/\tau_{sp}$ (where τ_{sp} is the spontaneous electron lifetime and L_n the electron diffusion length). From $\mu_n = 3000\,\mathrm{cm^2V^{-1}s^{-1}}$ for GaAs and $kT/e_0 = 26$ mV the electron diffusion constant $D_n = 78\,\mathrm{cm^2s^{-1}}$ for p doped GaAs is calculated. This value coincides well with the result calculated from $L_n = 5\,\mu$m for Ge-doped p-type GaAs layers [30] and $\tau_{sp} = 3$ ns. In highly doped GaAs the minority carrier diffusion constant can be smaller by more than an order of magnitude [23, 25]. The photon lifetime τ_{phi} in the i-th mode is given by [20]

$$\tau_{phi}^{-1} = \frac{c}{\bar{n}_i'}\left(\alpha_i' - \frac{1}{L}\ln R_i\right), \tag{5}$$

where α_i' is the internal optical loss per unit length, R_i the reflectivity of the end mirrors, both for the i-th mode and L is the laser length. For solution grown junctions at room temperature the photon lifetimes are between 1 and 2 ps [31].

The computational analysis of the single mode laser in many cases yields considerable insight into the laser dynamics. To some extent the results are also applicable to the physically more realistic multimode case. If only one mode oscillates, hole burning effects can be neglected and the spatial distribution of the electron and photon densities can be considered uniform within the active region. In this case the summation in (1) over i has to be deleted and $d^{-1}|\varphi(x,y)|^2$ has to be substituted by V^{-1}, in (2) the integrals over $|\varphi(x,y)|^2$ have to be replaced by 1. A further simplification of the mo-

nomode rate equations is possible by the following approximations

$$\varkappa^{-1} R_{sp}(n) \approx n/\tau_{sp} \tag{6}$$

$$\frac{\Gamma}{\Phi(E_s)} r_{sp}(E_s, n) \approx \frac{\alpha V n}{\tau_{sp}}. \tag{7}$$

Measured spontaneous electron lifetimes τ_{sp} of DHS lasers at room temperature are between 2 and 8 ns [32, 33]. The coefficient α, defined by (6, 7) gives the ratio of the spontaneous emission rate into the oscillating mode to the total spontaneous electron recombination rate. To give a rough estimate of the maximum value of α we set the internal quantum efficiency $\varkappa = 1$ and $R_{sp}(n)$ equal $r_{sp}(E_s, n)$ times the spontaneous emission line width. For $V/\Gamma = 10^{-9}\,\mathrm{cm}^3$, a spontaneous emission line width of 300 Å, and for the above calculated $\Phi(E_s) = 1.817 \times 10^{12}\,\mathrm{meV}^{-1}\,\mathrm{cm}^{-3}$ we obtain $\alpha = 1.07 \times 10^{-5}$. On the basis of Marinelli's approximation formula Adams has proposed a similar approximation for the stimulated emission coefficient

$$\frac{\Gamma}{V\Phi(E_s)} r_{st}(E_s, n) = g n^l, \tag{8}$$

where $l = 3$ for GaAs double heterostructure lasers at room temperature [22]. These approximations yield the rate equations

$$\frac{dn}{dt} = \frac{J}{e_0 d} - \frac{n}{\tau_{sp}} - g S n^l \tag{9}$$

$$\frac{dS}{dt} = -\frac{S}{\tau_{ph}} + \alpha V \frac{n}{\tau_{sp}} + V g S n^l. \tag{10}$$

For $\alpha = 0$ and $J \geqq J_{th}$ the explicit solution of the steady state rate equations is

$$n_{th} = \left(\frac{1}{V g \tau_{ph}}\right)^{1/l} \tag{11}$$

$$S = V \frac{\tau_{ph}}{\tau_{sp}} \left(\frac{1}{V g \tau_{ph}}\right)^{1/l} (J/J_{th} - 1), \tag{12}$$

where n_{th} is the threshold electron density at which the gain in the active region compensates the resonator losses. The threshold current density J_{th} is given by

$$J_{th} = e_0 d n_{th}/\tau_{sp}. \tag{13}$$

Figure 1 shownes the experimental light output versus current characteristics of two different injection lasers. Laser 1 shows a linear slope above threshold. The slope below threshold results from the spontaneous emission with a broad spectral distribution. The nonlinearity in curve 2 will be discussed later.

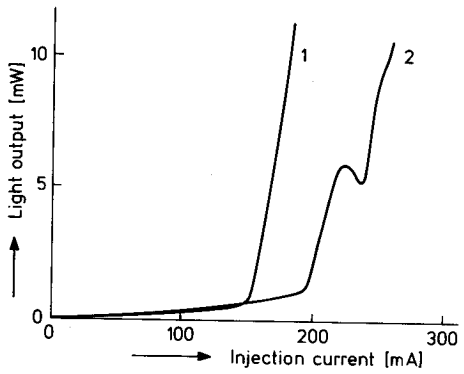

Fig. 1. Experimental light output versus current characteristics for two different injection lasers

2. Direct Modulation of Injection Lasers

If a step current pulse of amplitude I (the injection current I is given by the product of the injection current density J and the junction area) is applied to the laser, an initial delay time t_d passes until the onset of the laser oscillations and then the coherent emission starts with relaxation oscillations in the output power [34, 35]. The transient solution of the rate equations has been given by several authors [22, 36–39].

Figure 2a shows the transient response of a monomode injection laser to a step current pulse. We use the normalized electron density $z = n/n_{th}$, the normalized photon number $x = S\tau_{sp}/V n_{th} \tau_{ph}$ and the normalized injection current $\eta = I/I_{th} = J/J_{th}$. The laser parameters are $\tau_{sp}/\tau_{ph} = 10^3$, $l = 3$, $\alpha = 2 \times 10^{-5}$. The normalized step current pulse amplitude is $\eta = 1.1$. If a step current pulse of amplitude I is applied to an initially unbiased injection laser, the electron density in the active layer increases. As long as n is well below n_{th} no considerable amplification of the spontaneously emitted photons takes place. After the initial delay time [34, 35]

$$t_d = \tau_{sp} \ln [I/(I - I_{th})] \tag{14}$$

the electron density in the active layer reaches its threshold value and the photon number rises fast. As long as the photon number is below its stationary value, the electron density further increases above n_{th}. When S passes its stationary value, due to the rapidly increasing stimulated recombination processes the electron density quickly decreases but the photon number further increases until n passes again n_{th}. The fast decrease of the electron density continues up to the moment when the photon number falls below threshold. If the amplitude of the first photon spike is much higher than the stationary photon number, a considerable decrease of n

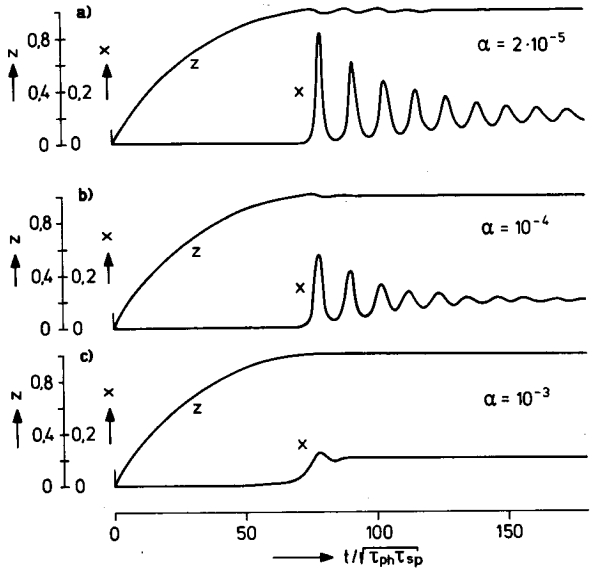

Fig. 2. Transient response of an injection laser to a step current pulse for different spontaneous emission contributions

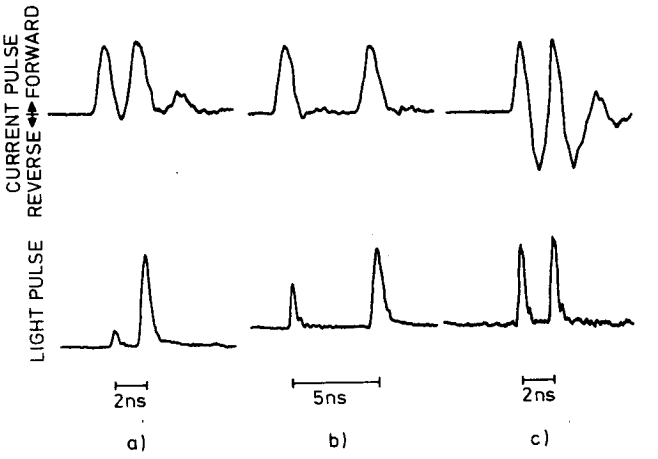

Fig. 3a–c. Current pulse (upper trace) and corresponding light pulse (lower trace) of a GaAs/GaAlAs DHS stripe geometry laser operated with double pulses with different pulse spacing (a) 2 ns, (b) 5 ns, and (c) 2 ns with pulses of forward and reverse swings; according to [42]

below n_{th} during the decrease of the light pulse takes place. Since the electron density is slowly raised again the photon number may decrease by several orders of magnitude until n has again reached n_{th}. Afterwards the whole process is repeated, but since the photon number in the considered mode now is higher than at the beginning of the process when n passed n_{th}, the photon number reaches its equilibrium value at a shorter time. Therefore the overshoot in the electron density and the following photon number overshoot are smaller than before. The process is repeated until the stationary state is reached.

For pulse modulation applications of injection lasers the delay time can easily be reduced by prebiasing the laser with a dc current I_0 [38, 40]. When a current pulse with amplitude I_p is superimposed the delay time is

$$t_d = \tau_{sp} \ln [I_p/(I_p - I_{th} + I_0)]. \quad (15)$$

If the laser is biased up to threshold, t_d vanishes.

If the laser is unbiased or biased below threshold and modulated with two subsequent pulses the delay time for the second pulse is reduced [34] since the electron density after the first current pulse is higher than before. In the case of direct pulse code modulation this would cause a pattern effect. Ozeki and Ito suggested the modulation of the injection laser by an additional compensation pulse before each modulation pulse which is preceded by a logical zero [41]. This compensation pulse is too small to generate a light pulse but raises the electron density up to the same level as a foregoing modulation pulse would have done. Two similar methods for pattern effect reduction have been shown by Lee and Derosier [42]. In the first case the modulation pulse amplitude is dependent on whether a modulation pulse preceded or not. In the second case the modulation signal consists of double pulses with a forward and a reverse swing (Fig. 3). The first forward swing causes the light pulse, whereas the second negative swing removes the excess charge in the active region. For prebiasing near threshold a pulse spacing of 2 ns is achieved without pattern effect.

With increasing contribution of spontaneous emission into the oscillating modes the damping of the relaxation oscillations is raised since the initial photon number in that case is higher, the stationary photon number is reached earlier and the overshoot consequently is smaller [37, 39, 43]. In the multimode case the relative contribution of spontaneous emission into the oscillating modes is proportional to the number of oscillating modes when the monomode calculation is taken as representative for the photon number in all oscillating modes. Figures 2b and c show calculations of the transient behaviour with $\alpha = 10^{-4}$ and $\alpha = 10^{-3}$. Angerstein and Siemensen deduced from measurements on DHS stripe-geometry injection lasers α as high as 5×10^{-4} [33]. Values of $10^{-3} < \alpha < 10^{-2}$ fitted to measurements on buried heterostructure lasers cannot be explained by such a strong spontaneous emission

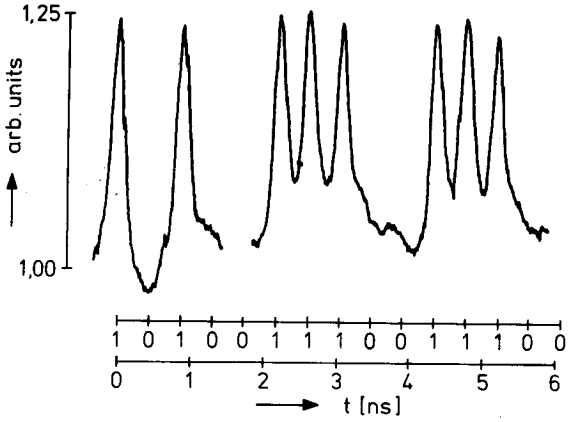

Fig. 4. Direct modulation of an injection laser at 2.3 Gbit/s

[44]. Pulse code modulation of injection lasers has been achieved up to more than 2 Gbit/s [45–49]. Figure 4 shows the direct modulation of an injection laser at 2.3 Gbit/s. Figure 5 shows the result of a 250 Mbit/s modulation experiment with a low mesa-stripe DHS injection laser [50]. When the laser is biased below threshold the light output shows a strong pattern effect. If the laser is biased 5% above threshold the pattern effect vanishes but the laser output exhibits a strong ringing, since every modulation pulse causes relaxation oscillations. We have seen that in the case of biasing below threshold pattern effects arise from the electron density dependence on a preceding pulse. In the case of biasing the laser above threshold the optical output pulse not only depends on the initial electron density in the active layer but also on the initial photon number in the oscillating modes. Danielsen has suggested to avoid pattern effects in Gbit/s PCM by biasing the laser approximately to threshold and giving the height and duration of the applied current pulses such values that the laser only emits the first spike of the relaxation oscillations and the electron and photon densities at the end of the current pulse return to their initial values [51]. In many experiments we have seen that in the case of pulse code modulation above 250 Mbit/s, when the laser is biased near threshold an exact adjustment of the bias current and the modulation amplitude is necessary. This can be well explained by the theory of Danielsen.

Sinusoidal modulation of injection lasers biased above threshold is a powerful tool for investigating the dynamic properties of injection lasers. Small signal analysis yields a resonance in the modulation depths versus modulation frequency curve [22, 52–54]. If I_1 is the complex modulation current amplitude and S_1 the

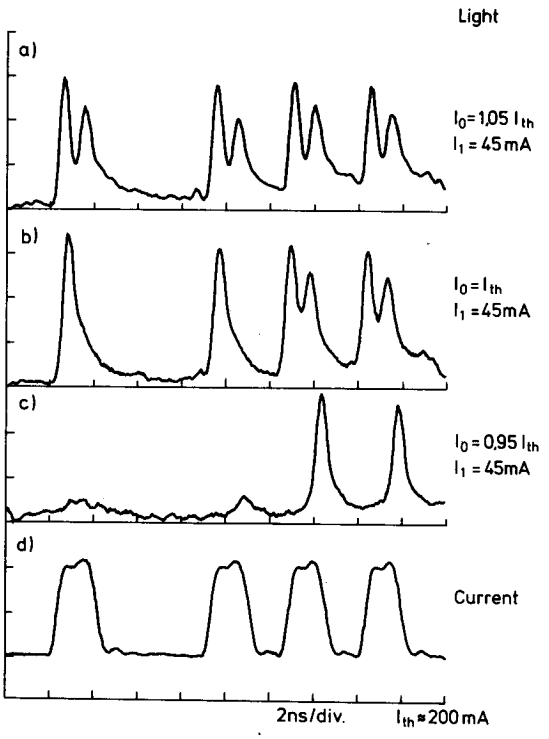

Fig. 5a–d. Direct modulation of an injection laser, at 280 Mbit/s and different bias currents

complex photon number amplitude, both at the angular frequency ω, and if the laser is biased to I_0 and S_0, respectively, we obtain by small-signal analysis of the rate equations (9, 10) for $\alpha = 0$

$$S_1/S_0 = (l/\tau_{sp}\tau_{ph}) \frac{I_1/I_0}{\omega_0^2 + j\omega\beta - \omega^2} \tag{16}$$

with

$$\omega_0^2 \tau_{sp}\tau_{ph} = l(I/I_{th} - 1) \tag{17}$$

and

$$\beta\tau_{sp} = l(I/I_{th} - 1) + 1. \tag{18}$$

Small-signal calculations including the effect of spontaneous emission have been performed by Harth and Siemsen [43]. Figure 6 shows the dependence of modulation depths on the modulation frequency for biasing 10% and 20% respectively, above threshold calculated from (9, 10) for $l = 3$ and $\alpha = 2 \times 10^{-5}$, 10^{-4}, 10^{-3}, 10^{-2}. The last three values of α are possible only in the case of many excited modes. The results of the small signal analysis suggest that a biasing of the injection laser much above threshold would be preferable

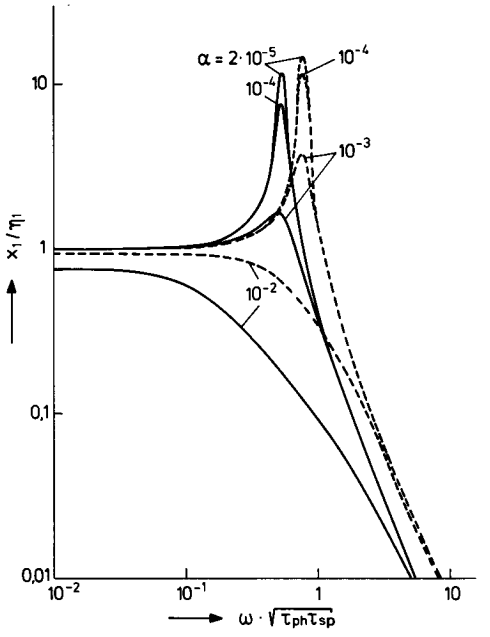

Fig. 6. Small signal modulation depths dependence on modulation frequency for biasing 10% (continuous curve) and 20% (broken curve) above threshold for $\tau_{sp}/\tau_{ph}=10^3$ and different α

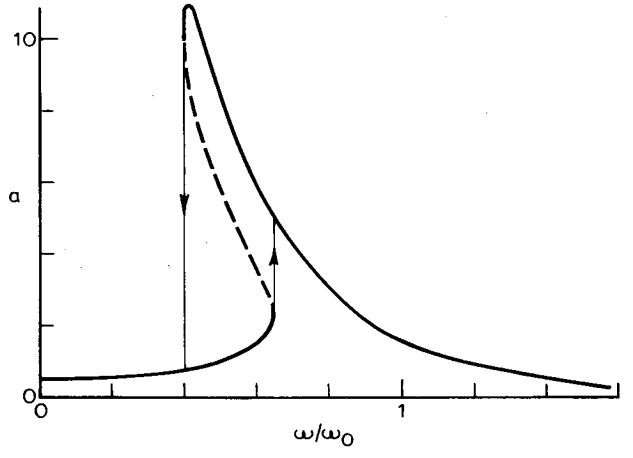

Fig. 7. Amplitude factor a as a function of the normalized modulation angular frequency. An unstable region (broken curve) leads to hysteresis phenomena ($\tau_{sp}/\tau_{ph}=50$, $\alpha=0$, $l=1$, $\eta_0=1.5$, $\eta_1=0.5$) [56]

for high frequency modulation. Unfortunately the laser there exhibits irregular phenomena which we shall discuss in the next two sections. Furthermore for optical communication applications a high dc light power level would also rise the shot noise in the receiver. The use of multimode lasers with a higher α is in contradiction with the narrow bandwidth requirements for low fiber dispersion.

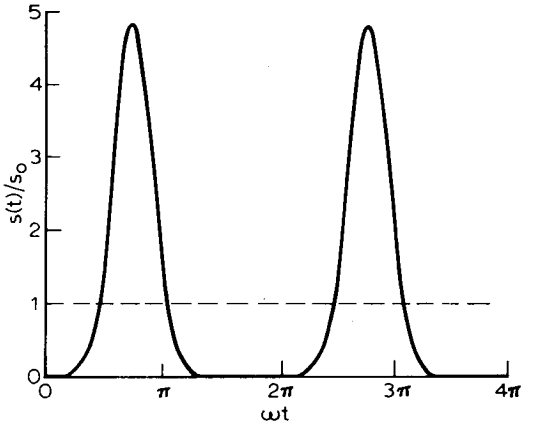

Fig. 8. Normalized photon density as a function of time [56]

When the laser is modulated by large sinusoidal currents the resonance frequency can be reduced considerably and the light output signal becomes distorted [55, 56]. With $l=1$ and $\alpha=0$ in (9, 10) according to [56] the analytical expression for the time dependence of the photon density is

$$S(t)=\frac{S_0}{\tilde{I}_0(a)}\exp\left[a\cos(\omega t+\theta)\right], \tag{19}$$

where $\tilde{I}_0(a)$ is the modified Bessel function of the first kind and of order zero, and a is an amplitude factor depicted in Fig. 7. At the large signal resonance frequency where $a\gg 1$ from (19) a pulse-like shape of the optical output signal arises (Fig. 8). We emphasize that this strong nonlinearity occurs although a completely linear dc light output versus current characteristic is assumed. This imposes restrictions on the application of amplitude modulation for high bandwidth fiber communication systems. The amplitude factor a has a maximum at threshold for which it yields a maximum modulation depth. Our experimental investigations of the large signal modulation depth as a function of the normalized bias current I_0/I_{th} confirm these theoretical results (Fig. 9). By generating spikes with a small sinusoidal current at the modulation resonance frequency and removing one or more light pulses by a short lowering of the bias, Schicketanz has demonstrated pulse code modulation at 650 Mbit/s [48].
Further investigations of the nonlinear rate equations have shown that by modulation at the double resonance frequency also subharmonics can be excited [57] and the small-signal modulation sensitivity can be increased by an additional large sinusoidal modulation current [58, 59].

3. Effect of Modulation on Spectrum and Nearfield

The dc spectral [9, 12, 29, 60] and nearfield [12, 61–63] behavior of injection lasers has been widely discussed. We have investigated the influence of modulation on the emission properties of injection lasers. Far below threshold, injection lasers exhibit a broad spontaneous emission spectrum (approximately 300 Å) which is narrowed with increasing current and exhibits a mode structure at and above threshold (Fig. 10). The laser can oscillate in a single or in a number of transverse modes and also in one or more filaments. The tendency to more filaments or to higher-order transverse modes increases with the stripe width of the active region and with the pumping above threshold. The latter increase is due to transverse spatial hole burning [25]. Each filament or transverse mode exhibits a longitudinal mode group. Since the gain spectrum of injection lasers has a broad maximum, also very small longitudinal hole burning should yield a number of longitudinal modes within the same transverse mode family. The envelopes of the longitudinal mode groups can be different in wavelength and intensity of the maximum. For the longitudinal modes the wavelength separation $\Delta\lambda$ of adjacent modes can be calculated from [29]

$$\Delta\lambda = \frac{\lambda_i^2}{2L\bar{n}_i'}. \tag{20}$$

For a typical laser length of 200–400 µm the longitudinal modes are separated by 1.5–3 Å. The transverse modes along the junction plane, however, have a separation in the order of 0.1 Å [9]. The spectral position of these lasing modes is very sensitive to temperature changes owing to two effects [12]. The band gap of a semiconductor decreases with increasing temperature. As a result the wavelength of the laser emission increases with temperature. This temperature coefficient is approximately 2.5 Å/K. In addition, the wavelength of an individual spectral mode has a temperature coefficient of approximately 0.4 Å/K because of the temperature dependence of the refractive index of the semiconductor [64]. To observe narrow spectral lines a careful temperature control of the laser is necessary. The temperature effects can influence the emission spectrum if the temperature of the junction region of the laser is increased in the course of the modulation pulse duration.

Many stripe-geometry DHS GaAs/GaAlAs lasers show nonlinearities—the so-called "kinks"—in the light output versus current characteristics [63, 65, 66]. Laser 2 in Fig. 1 shows a typical kink in the light output characteristic of a low mesa-stripe DHS injection laser with stripe width 25 µm. It has been found that these kinks are associated with filamentary structures of the nearfield intensity distribution parallel to the junction plane, spatial movement of the filaments within the stripe width, and excessive spectral broadening of the emission spectrum. Moreover, the location and character of the kinks can change during longtime operation of lasers. Until recently these kinks in the light output versus current curves have been a deleterious property of many lasers in respect of direct modulation of the

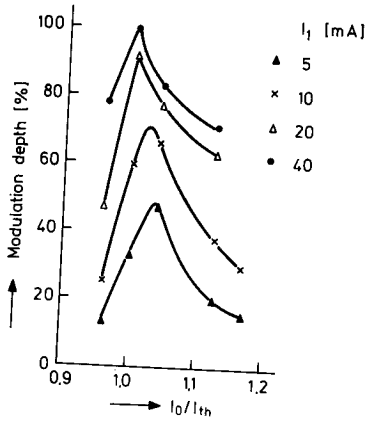

Fig. 9. Modulation depth as a function of the bias current I_0 for 280 MHz sinusoidal modulation at different modulation amplitudes I_1

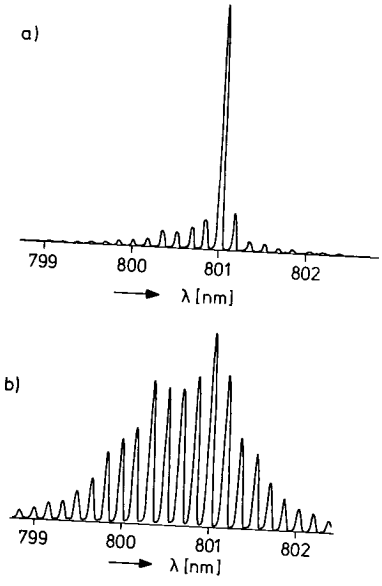

Fig. 10a and b. Emission spectrum of a low mesa-stripe GaAs DHS injection laser 3% above threshold (a) and close to threshold (b)

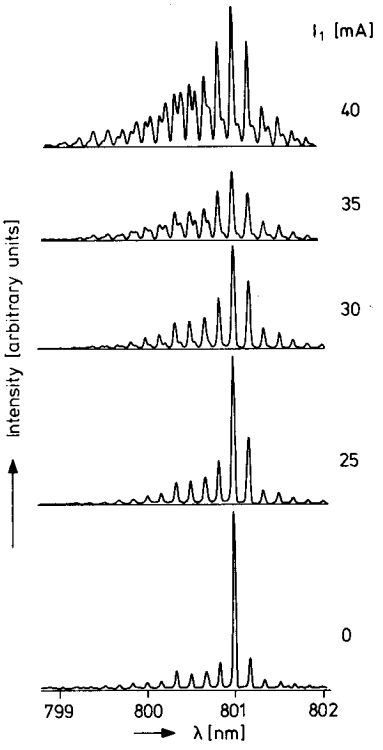

Fig. 11. Emission spectra of a GaAs laser directly modulated with the word 1000110001111100 at 300 Mbit/s and varying modulation current amplitude I_1. Bias current $I_0 = 130$ mA ($1.02\, I_{th}$)

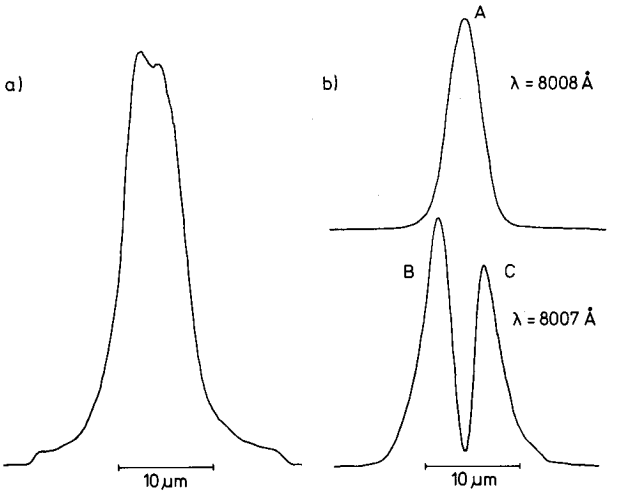

Fig. 12a and b. Nearfield intensity distribution along the junction plane of a GaAs laser operated with 300 Mbit/s PCM. Bias current $I_0 = 130$ mA, modulation current amplitude $I_1 = 40$ mA; (a) total near field; (b) monochromatic nearfields

laser light output. But recently, Dixon et al. [66] reported an improved linear light output versus current characteristic by reducing the excited stripe width of the active region of the DHS GaAlAs lasers below 10 μm, whereas lasers with a stripe width ranging from 10–20 μm show reproducible kinks [67]. In narrow stripe lasers the kinks move to a higher current range and may occur again at higher light output power.

Experimental investigations show that high-frequency direct modulation causes an intensity decrease of dominant modes while the number of neighbouring longitudinal modes is increased. Consequently the spectral envelope is broadened [68–70]. When the injection current is modulated, also the electron density oscillates with the modulation frequency. The electron density modulation amplitude increases with the modulation current amplitude and also with the modulation frequency. If the electron density oscillates there are periods when modes with a higher threshold electron density may have a net gain and the number of oscillating modes is increased. As the total number of photons is injection-limited, by the increase of the number of modes the intensity of the dominant mode is reduced. Figure 11 shows the effect of 300 Mbit/s pulse code modulation on the emission spectrum of a GaAs low mesa-stripe DHS injection laser. The quasi single mode emission of the laser without modulation changes with increasing modulation current to a multimode emission. Besides the increase of the number of longitudinal modes a new mode family appears.

For the interpretation of the spectral change the modulation influenced emission spectrum has been investigated spatially and time resolved. Figure 12a shows the integral intensity distribution of the nearfield along the junction plane and Fig. 12b the corresponding monochromatic nearfield distributions of neighbouring modes belonging to different longitudinal mode families. The nearfield distribution A belongs to the fundamental transverse mode and the intensity distribution B/C exhibits the first-order transverse mode. The spatially resolved emission spectra at the nearfield positions A, B, and C are shown in Fig. 13 together with the integral emission spectrum. As can be seen, the fundamental transverse mode (A) yields a quasi single mode emission spectrum which is essentially the same as the spectrum without modulation (Fig. 11). At the positions B and C of the first-order transverse mode an identical spectrum is measured, but it is different from the spectrum at position A. The peak wavelength is 4.5 Å shorter than in the spectrum of the fundamental transverse mode. The lower wavelength

for the first-order mode is in agreement with the measurements of Buus et al. [25] and in contradiction to their theoretical considerations. The wavelength shift can probably be explained by higher bandfilling caused by the modulation current pulses.

In order to investigate the dynamic behaviour of the emission of the modulated laser, the time resolved light pulses have been measured. In Fig. 14 the light pulses of the five figures "1" of the word 1000110001111100 at 300 Mbit/s are shown for the same modulation conditions as for the spatially resolved spectra. Besides the light pulses for the overall intensity distribution also the light pulses for the fundamental (A) and first-order (B, C) transverse modes are measured. The light pulses show spikes caused by relaxation oscillations. The first spike of the relaxation oscillations is lasing in the fundamental mode (A) in agreement with the results of [25]. The first-order transverse mode (B, C) is excited later, as can be seen from Fig. 14. Measurements of the time resolved spectra have yielded essentially the quasi single mode emission spectrum of Fig. 11 in the first spike of the light pulse and the modulation induced spectrum with the shorter peak wavelength exhibited by the first-order mode is observed in the following spikes of the light pulse. The results of these investigations show that for certain modulation conditions it may be possible to retain the emission spectrum unchanged in spite of direct modulation of the laser, provided that the modulation pulses are very short or the light pulse is suppressed after the first spike of the relaxation oscillation. By appropriate choice of pulse amplitude and duration direct Gbit/s-modulation free of pattern effects and spectral broadening is possible [71, 72]. However, the need of an accurate bias and pulse amplitude control would complicate technical applications of this method.

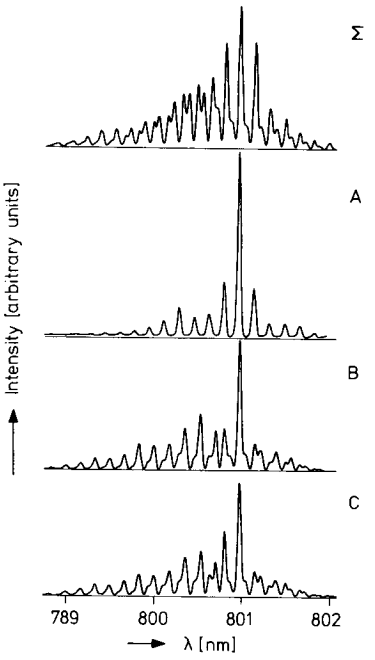

Fig. 13Σ–C. Spatially resolved emission spectra of the GaAs laser operated as in Fig. 12. (Σ): Emission spectrum of the total light output, (A): Emission spectrum of the fundamental transverse mode, and (B), (C): Emission spectrum of the first order transverse mode

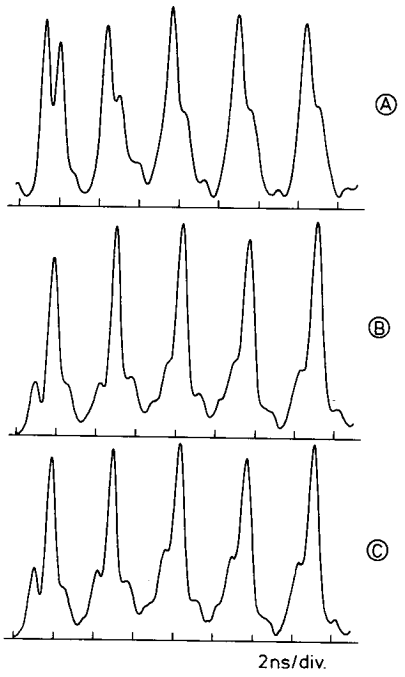

Fig. 14A–C. Time resolved light output of the laser operated as in Fig. 12. Light pulses of the five "1" of the word 1000110001111100. (A): Light pulses in the fundamental transverse mode, and (B), (C): Light pulses in the first order mode

4. Spontaneous Fluctuations

From (17) and (18) can be seen that the modulation bandwidth of injection lasers increases with bias level. Unfortunately injection lasers tend to exhibit stationary spontaneous fluctuations when they are dc biased to more than a few per cent above threshold [68, 73–76]. The frequency of these spontaneous fluctuations has a range from 0.1 to a few GHz and coincides with the modulation resonance frequency for sinusoidal modulation. As the modulation depths can take values up to 80% [77] this effect is a severe limitation for high frequency direct modulation of injection lasers. Several theoretical models have been

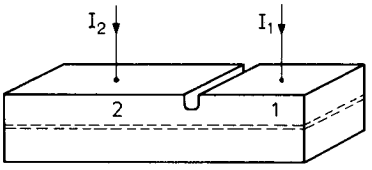

Fig. 15. Double section injection laser

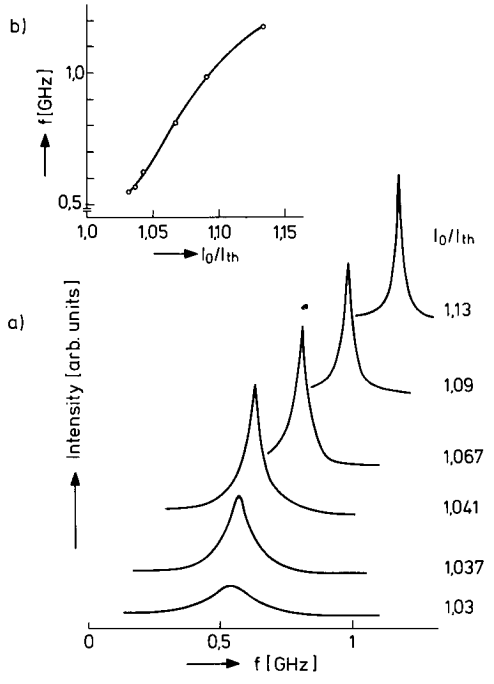

Fig. 16. (a) Frequency spectrum of spontaneous fluctuation of a cw operated low mesa-stripe GaAs/GaAlAs laser for different injection currents. (b) Fluctuation frequency as a function of the normalized injection current I_o/I_{th}

proposed for a physical understanding of the spontaneous fluctuations.

Basov et al. [73, 78] supposed spatial inhomogeneities to be the reason for the spontaneous fluctuations. The influence of spatial inhomogeneities on the laser dynamics has been treated by the simple theoretical model of a laser divided into two sections 1 and 2 (Fig. 15). The gain in the two sections can be controlled separately by the injection currents I_1 and I_2. Both active regions are within the same Fabry-Perot resonator. To achieve laser action it is sufficient that only one of the sections exhibits optical gain. In the diode which is only biased in the lossy region a photon field in the resonator raises the electron level, whereas in the diode, which exhibits optical gain, the electron density is lowered by a photon field. Now if the absorbing section saturates faster than the amplifying one, there exists a region of photon number where the net optical amplification in the Fabry-Perot resonator increases with the photon number and the steady state solution of the laser rate equations becomes unstable.

If r_{st1} and r_{st2} are the stimulated emission coefficients in sections 1 and 2, and γ is the ratio of the volume of section 2 to that of section 1 the condition of instability is

$$r_{st1}\frac{\partial r_{st1}}{\partial n_1}+\gamma r_{st2}\frac{\partial r_{st2}}{\partial n_2}<0. \tag{21}$$

By this model possible fluctuations can be explained in all laser structures where the photon field can couple to lossy semiconductor regions with a band gap smaller than the photon energy.

Kobayashi has shown experimentally and theoretically that stationary fluctuations can arise when two parallel lasers are optically coupled [79]. In the same way spontaneous fluctuations could also be caused by the coupling of two filaments or two mode groups with different transverse mode structure. The theory of Kobayashi is on the basis of the rate equations and includes no mode locking phenomena, where the pulsation frequency is related to the difference of oscillating frequencies of interacting modes. Ordinary mode locking would yield spiking frequencies in the order of 10^{11} Hz. Therefore second-order mode locking has been proposed for injection lasers [68, 74, 81]. Although [81] brings experimental evidence for second-order mode locking, the measured fluctuation behavior of lasers with a narrow emission spectrum [76] can rather be explained by the theory of Basov. We think that the Q-switching, proposed by Basov is the main reason for spontaneous self-pulsing phenomena. These phenomena are surely influenced and possibly also enhanced by mode or filament interactions.

We have measured the microwave spectrum of the spontaneous optical output pulsations of dc operated low mesa-stripe geometry DHS GaAs injection lasers. Figure 16 shows the typical decrease of the rf bandwidth of the output pulsations and the increase of the fluctuation frequency and amplitude with increasing injection current. Generally we observed that an abrupt change in the fluctuation frequency is always accompanied by a change in the filamentary structure of the nearfield intensity distribution [82].

An emission spectrum without (Fig. 17a) and with (Fig. 17b) fluctuation is shown for the same laser at different injection levels. Fluctuations cause a broadening of the

spectral envelope of the longitudinal modes and also a broadening of the individual modes as can be obviously seen from the intersections in Fig. 17. The linewidth widens by a factor two.

The broadening of the spectral lines can be explained in the following way. The spontaneous fluctuations cause an oscillation of the electron density and therewith also an oscillation of the refractive index in the active region and a corresponding oscillation in the wavelength shift. In the time averaged measurement this effect shows a spectral broadening. In spontaneously pulsating injection lasers the spectral broadening of the emission spectrum is the same as in the case of direct modulated injection lasers.

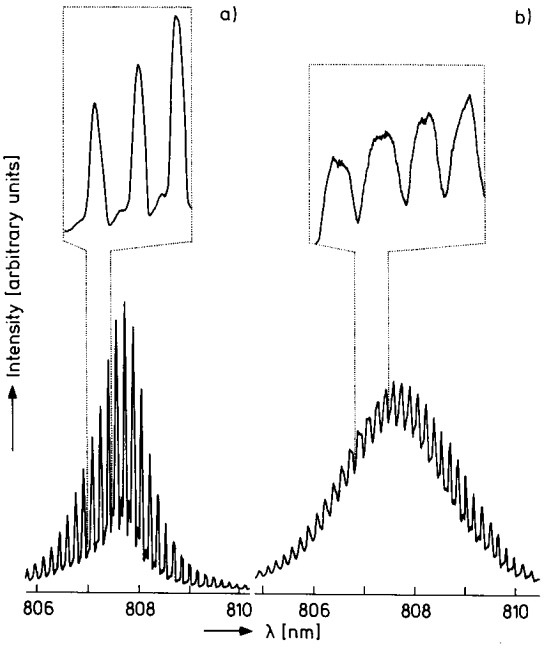

Fig. 17a and b. Longitudinal-mode spectra of a cw operated low mesa-stripe GaAs/GaAlAs laser: (a) Laser operation without spontaneous fluctuation ($I_0 = 214\,\text{mA}$). (b) Laser operation with spontaneous fluctuation ($I_0 = 283\,\text{mA}$)

5. Coupled Laser Structures

Optically coupled injection lasers exhibit very interesting modulation and spectral properties. Depending on the strength of coupling quite different effects can be observed.

Strong optical coupling is achieved when both laser systems are within the same Bragg resonator or very close by aligned end to end [16, 78, 83]. We have discussed such a system in the preceding section. For inhomogeneous excitation there also exist points of operation where such junctions exhibit a bistable switching behavior. Applications can be seen for pulse shaping and optoelectronic logic AND gates.

Another promising application of optically coupled injection lasers is to improve the modulation performance of injection lasers. It has been shown theoretically and experimentally, that the modulation bandwidth of an injection laser can be increased by injection of a coherent light signal into one of its oscillating modes [84–90]. In the second section we have shown that a high initial photon number in the oscillating modes causes a strong damping of the relaxation oscillations. By injection of a coherent light signal into one oscillating mode of an injection laser this strong damping occurs without multimode operation. Figure 18 shows the experimentally observed optical response of an injection laser to a step current pulse [90]. The computer simulation of a 2 Gbit/s direct pulse code modulation of a multimode injection laser has shown that by coherent light injection not only the pattern effects are eliminated but also the nonirradiated modes are suppressed [86] (Fig. 19). The suppression of the nonirradiated modes results from the electron density and therefore gain lowering in the active layer, caused by the light injection. Practically coherent light

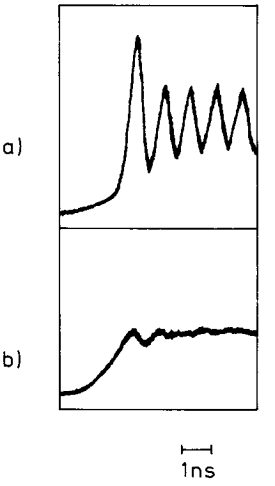

Fig. 18a and b. Response of an injection laser to a step current pulse with an amplitude approximately 3% above threshold without (a) and with (b) coherent light injection

injection at the center wavelength of a mode is impossible and there is always a detuning between the wavelength of the injected radiation and the wavelength of the free-running laser mode. The locking range for synchronization to the wavelength of the

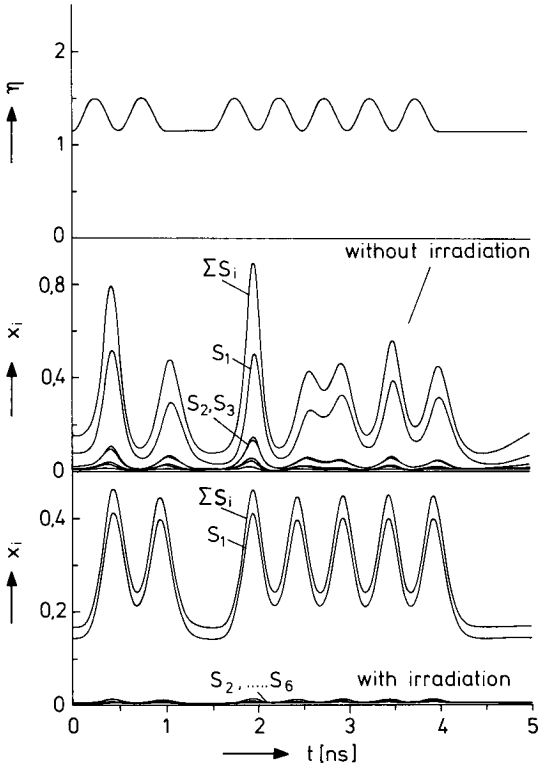

Fig. 19. Normalized photon numbers $x_i = S_i \tau_{sp}/V n_{th} \tau_{ph}$ and normalized modulation current $\eta = I/I_{th}$ as a function of time without and with coherent light injection

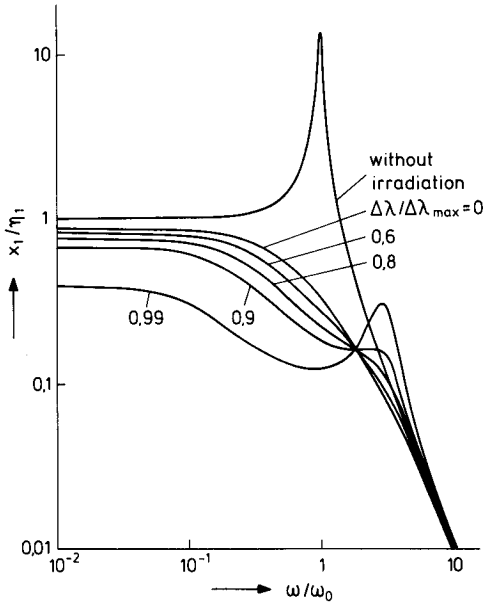

Fig. 20. Small signal modulation depths versus modulation frequency characteristic with and without coherent irradiation for different ratios of the wavelength detuning range $\Delta\lambda$ to the wavelength locking range $\Delta\lambda_{max}$ ($\tau_{sp}/\tau_{ph} = 10^3$, $l = 3$, $\eta_0 = 1.1$)

injected radiation is proportional to the amplitude ratio of injected radiation and radiation produced in the laser and inversely proportional to the laser length [89, 90]. For an amplitude ratio of 10^{-2} a locking range of more than 0.1 Å can be achieved [90]. If two lasers with different longitudinal mode spacing are coupled, by appropriate choice of the laser parameters there always exist one or more pairs of modes with sufficiently close wavelengths to insure locking [89, 91].

Figure 20 shows the small signal modulation depths versus modulation frequency characteristics with and without coherent light injection [90]. The calculations with coherent light injection have been performed for different detuning $\Delta\lambda$ between the wavelength of the injected radiation and the free-running wavelength of the laser mode. When the detuning is smaller than the locking range, the resonance in the modulation characteristics vanishes. Figure 21 shows the large signal response to a step pulse which changes I/I_{th} from 0.9 to 1.1 at the time $t = 0$ [90]. With light injection the response is strongly damped within the whole locking range and exhibits no spiking response. For a detuning larger than the stationary locking range the frequency locking breaks down and the laser produces strong spiking oscillations. The frequency of these spiking oscillations is identical with the difference between the frequencies of the free running mode and the incident radiation. This modulation by coherent light injection has also been experimentally observed [92].

6. Outlook

Although stripe-geometry DHS GaAs injection lasers under certain experimental conditions can be modulated up into the GHz region there are still problems to be solved for a technical application. The spontaneous fluctuations can possibly be eliminated when laser structures can be developed where the optical field does not reach into absorbing regions with a band gap smaller than the photon energy.

Since the multimode emission structure is caused by spatial hole burning and the hole burning is intensified by a low minority carrier mobility, undoped active layers with a very good crystal perfection should be used. Another possibility to obtain a stable longitudinal single mode output is the distributed feedback injection laser [93].

Theoretical investigations yield for distributed feedback injection lasers the same modulation behavior as for Fabry-Perot type monomode lasers [94]. Single

41. T.Ozeki, T.Ito: IEEE J. Quant. Electr. QE-**9**, 1098–1101 (1973)
42. T.P.Lee, R.M.Derosier: Proc. IEEE **62**, 1176–1177 (1974)
43. W.Harth, D.Siemsen: Arch. Elektron. Übertragungstech. **30**, 343–348 (1976)
44. T.Kobayashi, S.Takahashi: Japan J. Appl. Phys. **15**, 2025–2026 (1976)
45. M.Chown, A.R.Goodwin, D.F.Lovelace, G.H.B.Thompson, P.R.Selway: Electron. Lett. **9**, 34–36 (1973)
46. H.W.Thim, L.R.Dawson, J.V.Di Lorenzo, J.C.Dyment, C.J.Hwang, D.L.Rode: 1973, Int. Solid-State Circuits Conf. Digest of Technical Papers (1973) pp. 92–93
47. P.Russer, S.Schulz: Arch. Elektron. Übertragungstech. **27**, 193–195 (1973)
48. D.Schicketanz: Siemens Forsch.- und Entw. Ber. **2**, 218–221 (1973)
49. H.Yanai, M.Yano, T.Kamiya: IEEE J. Quant. Electr. Qu-**11**, 519–524 (1975)
50. P.Marten, to be published
51. M.Danielsen: IEEE J. Quant. Electr. QE-**12**, 657–660 (1976)
52. T.Ikegami, Y.Suematsu: Electron. Commun. Japan **51**, 51–57 (1968)
53. T.Ikegami, Y.Suematsu: Proc. IEEE **55**, 122–123 (1967)
54. F.L.Paoli, J.E.Ripper: Proc. IEEE **58**, 1457–1465 (1970)
55. T.Ikegami, Y.Suematsu: Electron. Commun. Japan **53**-B, 69–75 (1970)
56. W.Harth: Electron. Lett. **9**, 532–533 (1973)
57. W.Harth, D.Siemsen: Arch. Elektron. Übertragungstechn. **28**, 391–392 (1974)
58. P.Russer, H.Hillbrand, W.Harth: Electron. Lett. **11**, 87–89 (1975)
59. H.Grothe, W.Harth, P.Russer: Electron. Lett. **12**, 522–524 (1976)
60. S.Iida, Y.Watanabe: Jap. J. Appl. Phys. **13**, 1249–1258 (1974)
61. J.E.Ripper, F.D.Nunes, N.B.Patel: Appl. Phys. Lett. **27**, 328–330 (1975)
62. B.W.Hakki: IEEE J. Quant. Electr. QE-**11**, 149–154 (1975)
63. T.L.Paoli: IEEE J. Quant. Electr. QE-**12**, 770–776 (1976)
64. C.H.Gooch: *Injection Electroluminescent Devices* ((Wiley, London 1973) pp. 138–142
65. T.L.Paoli, P.A.Barnes: Appl. Phys. Lett. **28**, 714–716 (1976)
66. R.W.Dixon, F.R.Nash, R.L.Hartman, R.T.Happlewhite: Appl. Phys. Lett. **29**, 372–374 (1976)
67. K.Kobayashi, R.Lang, H.Yonezu, J.Sakuma, I.Hayashi: Jap. J. Appl. Phys. **16**, 207–208 (1977)
68. T.L.Paoli, J.E.Ripper: Phys. Rev. Lett. **22**, 1085–1088 (1969)
69. T.Ikegami: Proc. 1st European Conf. Opt. Commun. London (Sept. 1975) pp. 111–113
70. D.Siemsen, J.Angerstein: Electron. Lett. **12**, 432–434 (1976)
71. P.R.Selway, A.R.Goodwin: Electron. Lett. **12**, 25–26 (1976)
72. W.Freude: University Karlsruhe, reported at the DFG-meeting "Optical Communication" (March 1977, Berlin) single-mode emission of an injection laser, directly modulated at 264 Mbit/s
73. N.G.Basov, V.N.Morozov, V.V.Nikitin, A.S.Semenov: Sov. Phys. Semicond. **1**, 1305–1308 (1968)
74. T.P.Lee, R.Roldan: IEEE J. Quant. Electron. QE-**5**, 551–552 (1969)
75. T.L.Paoli, J.E.Ripper: Appl. Phys. Lett. **18**, 466–468 (1971)
76. N.Chinone, R.Ito: Japan. J. Appl. Phys. **13**, 575–576 (1974)
77. T.L.Paoli: IEEE J. Quant. Electron. QE-**13**, 351–359 (1977)
78. N.G.Basov: IEEE J. Quant. Electron. QE-**4**, 855–864 (1968)
79. K.Kobayashi: IEEE J. Quant. Electron. QE-**9**, 449–457 (1973)
80. H.-G. Wöhrstein, H.Haken: IEEE J. Quant. Electron. QE-**9**, 318–323 (1973)
81. J.E.Ripper, T.L.Paoli: IEEE J. Quant. Electron. QE-**8**, 74–79 (1972)
82. G.Arnold, K.Petermann: Self-pulsing phenomena in injection lasers (to be published)
83. A.B.Fowler: J. Appl. Phys. **35**, 2275–2276 (1964)
84. P.Russer: Arch. Electron. Übertragungstech. **29**, 231–232 (1975)
85. P.Russer: Laser 75 Optoelectron. Conf. Proc. München (May 1975) pp. 161–164
86. H.Hillbrand, P.Russer: Electron. Lett. **11**, 372–374 (1975)
87. R.Lang, K.Kobayashi: IEEE J. Quant. Electron. QE-**11**, 60D (1975)
88. K.Kobayashi, R.Lang, K.Minemura: Proc. 1st European Conf. Opt. Commun. London (Sept. 1975) pp. 138–140
89. R.Lang, K.Kobayashi: IEEE J. Quant. Electron. **12**, 194–199 (1976)
90. P.Russer, G.Arnold, K.Petermann: High-speed modulation of DHS lasers in the case of coherent light injection (to be published in Proc. 3rd European Conf. on Opt. Commun., München, Sept. 1977)
91. R.Salathé, C.Voumard, H.Weber: Phys. Stat. Sol. (a) **23**, 675–682 (1974)
92. J.-I.Nishizawa, K.Ishida: IEEE J. Quant. Electron. QE-**11**, 515–519 (1975)
93. M.Nakamura, K.Aiki, J.Umeda, A.Yariv: Appl. Phys. Lett. **27**, 403–405 (1975)
94. S.R.Chinn: Opt. Commun. **19**, 208–211 (1976)
95. H.Namizaki: IEEE J. Quant. Electron. QE-**11**, 427–431 (1975) H.Namizaki: Trans. IECE of Japan, E **59**, 8 (1976)
96. T.Tamir: Integrated Optics (Springer, Berlin, Heidelberg, New York 1975)
97. D.N.Payne, W.A.Gambling: Electron. Lett. **11**, 176–178 (1975)